



Functional organization of the primary auditory cortex of the free-tailed bat *Tadarida brasiliensis*

Silvio Macias¹ · Kushal Bakshi¹ · Michael Smotherman¹

Received: 8 November 2019 / Revised: 20 January 2020 / Accepted: 22 January 2020 / Published online: 8 February 2020
© Springer-Verlag GmbH Germany, part of Springer Nature 2020

Abstract

The Mexican free-tailed bat, *Tadarida brasiliensis*, is a fast-flying bat that hunts by biosonar at high altitudes in open space. The auditory periphery and ascending auditory pathways have been described in great detail for this species, but nothing is yet known about its auditory cortex. Here we describe the topographical organization of response properties in the primary auditory cortex (AC) of the Mexican free-tailed bat with emphasis on the sensitivity for FM sweeps and echo-delay tuning. Responses of 716 units to pure tones and of 373 units to FM sweeps and FM–FM pairs were recorded extracellularly using multielectrode arrays in anesthetized bats. A general tonotopy was confirmed with low frequencies represented caudally and high frequencies represented rostrally. Characteristic frequencies (CF) ranged from 15 to 70 kHz, and fifty percent of CFs fell between 20 and 30 kHz, reflecting a hyper-representation of a bandwidth corresponding to search-phase echolocation pulses. Most units showed a stronger response to downward rather than upward FM sweeps and forty percent of the neurons interspersed throughout AC (150/371) showed echo-delay sensitivity to FM–FM pairs. Overall, the results illustrate that the free-tailed bat auditory cortex is organized similarly to that of other FM-type insectivorous bats.

Keywords Auditory cortex · Tonotopy · FM sweep direction · Echo-delay tuning · *Tadarida*

Abbreviations

AC	Auditory cortex
CD	Characteristic delay
CF	Characteristic frequency
CF-FM	Constant-frequency–frequency-modulated pulses
DRA	Delay response area
DSI	Direction selectivity index
FM	Frequency modulated
FRA	Frequency response area
MT	Minimum threshold
PSTH	Post-stimulus time histogram

Introduction

The auditory cortex of echolocating bats follows the general plan for mammals except that it is comprised of neuronal subtypes and functional areas that encode acoustic cues

uniquely related to biosonar processing. Echolocating bats are commonly segregated into those that emit pulses composed of downward frequency-modulated (FM) sweeps versus those that use some combination of constant-frequency and FM components. Bats that use CF-FM pulses, such as the horseshoe bats and mustached bats display auditory cortices with multiple spatially segregated specialized subfields, including a tonotopically organized primary auditory field (A1), an area consisting of echo-delay-tuned neurons that are arranged chronotopically to map target range, and also an area that maps target velocity relative to the bat (O'Neill 1995). FM bats also possess echo-delay-tuned neurons but differ from CF-FM bats in that they are found interspersed within the primary auditory field (Kössl et al. 2014, 2015), and while no relative velocity areas have yet been reported, they possess combination-sensitive neurons that respond preferentially to complex echo acoustic patterns related to target shape and size (Dear et al. 1993a; Sanderson and Simmons 2002). The functional significance of the various echolocation-related neuronal response properties and auditory subfields may be self-evident, but it remains a mystery as to how the auditory cortex in bats or any other mammal reintegrates the parcellated acoustic cues represented by the auditory cortex subfields to reconstruct the auditory scene.

✉ Silvio Macias
smacias@bio.tamu.edu

¹ Department of Biology, Texas A&M University,
College Station, TX 77843, USA

Comparative studies can provide critical insights towards this, but to date a comprehensive mapping of the functional organization of AC has been completed for only a few bat species (Kössl et al. 2014, 2015), and from among those only two FM-type insectivorous bats, the big brown bat *Eptesicus fuscus* (Jen et al. 1989; Dear et al. 1993a, b) and the little brown bat *Myotis lucifugus* (Wong and Shannon 1988), both from the family Vespertilionidae.

This study provides the first neurophysiological survey of the topographical organization of response properties in primary auditory cortex of the Mexican free-tailed bat (*Tadarida brasiliensis*), an FM-type insectivorous bat from the family Molossidae. The biosonar behavior and pulse acoustics of *T. brasiliensis* appear very similar to those of the big brown bat *E. fuscus*, but *T. brasiliensis* also displays many behavioral and morphological specializations for hunting prey at high speeds and high altitudes. While echolocating in transit or open spaces, *T. brasiliensis* use relatively long and shallow frequency-modulated (FM) “search” calls, which are replaced by a series of progressively steeper linearly frequency-modulated FM “approach” calls whenever the bat approaches a target or obstacle (Simmons et al. 1978). An example approach sequence of *Tadarida* is shown in Fig. 1a. Their communication calls are also of interest, due to their variable durations and diverse spectrotemporal designs including downward, upward, and sinusoidally modulated FM sweeps (Ma et al. 2004; Schwartz et al. 2007; Bohn et al. 2008). The repertoire of social calls uttered by the Mexican free-tailed bat is elaborate and the behavioral contexts in which the different vocalizations are used have been well documented (Ma et al. 2004; Schwartz et al. 2007; Bohn et al. 2008), which helped make *T. brasiliensis* a successful animal model for studying the cellular and synaptic mechanisms of auditory processing in the brainstem and midbrain (Pollak et al. 2003; Andoni et al. 2007). However, so far nothing is known about their auditory neurophysiology above the inferior colliculus. Here, we report the results of our study using microelectrode arrays in anesthetized free-tailed bats characterizing and mapping the response properties of neurons within the primary auditory cortex in the dimensions of frequency representation, selectivity for direction of FM sweeps and tuning to call echo delay.

Materials and methods

Animals

Electrophysiological recordings from the AC were performed in eight adult (five females, three males) Mexican free-tailed bats, *Tadarida brasiliensis*. Animals were group-housed in an artificial habitat at Texas A&M University (TAMU) with a reversed light cycle.

Surgical procedures

All animals were anesthetized with a solution of sodium pentobarbital (80 mg/kg, Euthasol, Virbac AH, Inc., Texas, USA) and positioned within a custom-built stereotaxic apparatus. Body temperature was maintained within normal ranges using a heating lamp. The skin and temporal muscles overlying the skull were cut and removed and a custom-fabricated post was attached to the bone at the midline using cyanoacrylate gel. A craniotomy (~2×2 mm) was made using a scalpel blade to expose the left auditory cortex.

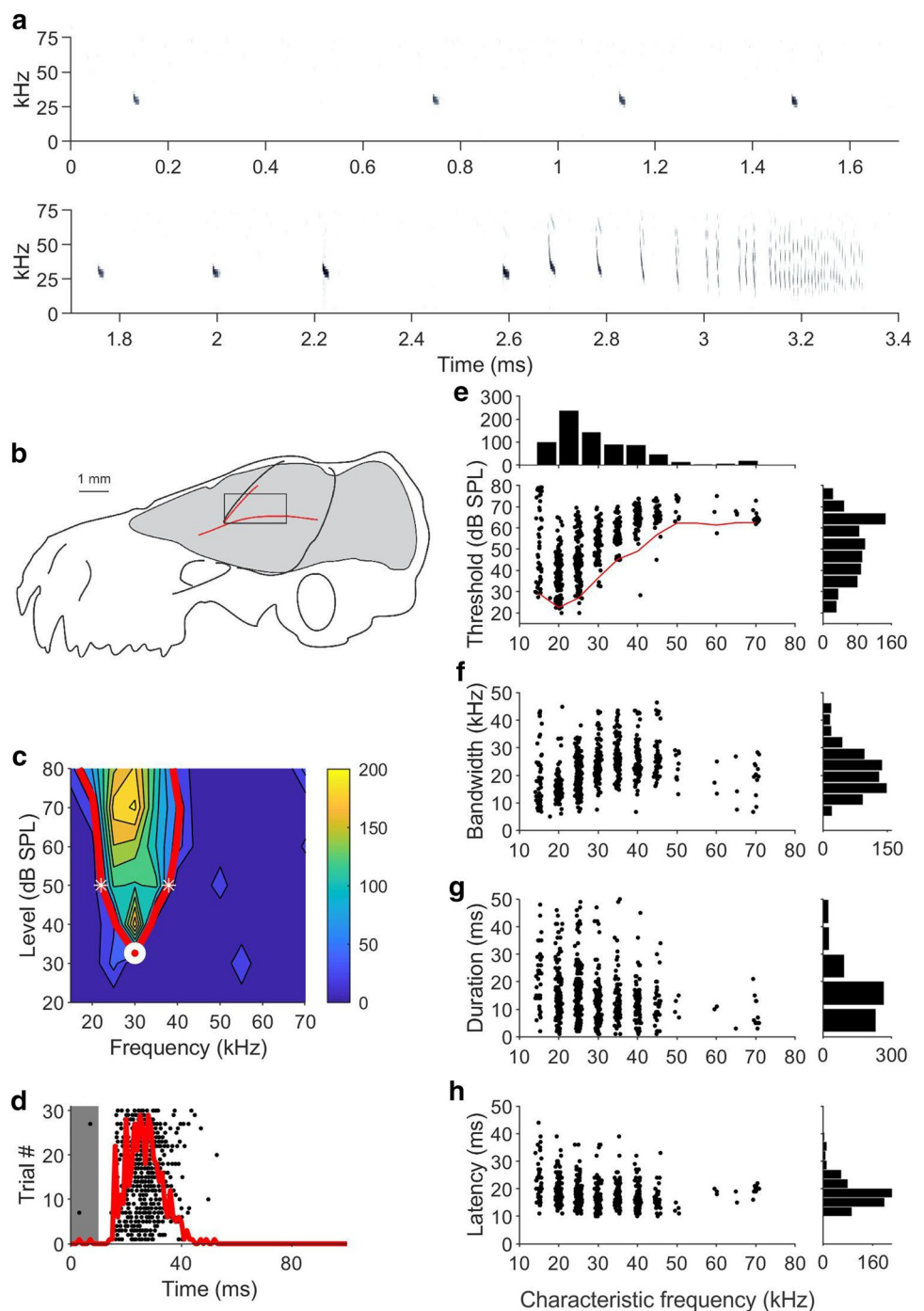
Acoustic stimuli

Pure tones were digitally synthesized and controlled using a custom-written program in Matlab (R2018a, MathWorks, Natick, MA, USA). Acoustic stimuli were generated at a sampling rate of 250 kHz with a National Instruments card (NI USB-6356). The audio signal was transferred to an audio amplifier (SONY, STR-DE197). The acoustic stimuli were broadcast to the bat with a calibrated speaker (DaytonAudio, PTMini-6) centered directly in front of the head and 10 cm from the bat’s ear. The calibration curve was obtained with a Brüel and Kjaer sound recording system (1/4-inch Microphone 4135, Microphone Preamplifier 2670, Brüel and Kjaer, Naerum, Denmark) connected to a conditioning microphone amplifier (Nexus 2690, Brüel and Kjaer, Naerum, Denmark).

To measure the frequency response area, we presented the animal with a pseudorandomized series of pure tones (10 ms duration, 0.5 ms rise/fall time) at different sound pressure levels (step size 10 dB, range 20–80 dB SPL) and frequencies (step size 5 kHz, range 15–70 kHz). Each frequency-level combination was presented 30 times at an interval of 300 ms. To test for FM sweep directional selectivity, we recorded responses to downward and upward FM sweeps of 50 kHz bandwidth (between 20 and 70 kHz) over a range of different durations (1, 2, 3, 5, 10, 25 and 50 ms). All FM sweeps were broadcasted at a RMS level of 80 dB SPL and presented 30 times at an interval of 300 ms.

For characterization of the call-echo delay selectivity, we presented the bat with two downward FM sweeps of 2 ms duration. The temporal position and amplitude (80 dB SPL) of the first sweep (call) was held constant, whereas the temporal position and RMS level of a second sweep (echo) were randomly changed. For example, in a typical recording, the call onset was set at the beginning of the recording window and the onset of the echo was randomly changed between 4, 6, 8, 12, 16, 24, 30 and 50 ms. RMS level of the echo varied from 10 to 70 dB SPL in 10 dB steps. Each FM–FM pair was presented 20 times at an interval of 300 ms.

Fig. 1 Echolocation of *Tadarida brasiliensis* and location and basic response properties of the primary AC. **a** Example of echolocation sequence emitted by the Mexican free-tailed bat during insect pursuit. **b** Location of the primary auditory cortex. The location of the median cerebral artery and its branches were used as reference points. **c** Example of a frequency response area and the corresponding frequency tuning curve. White open circle indicates the characteristic frequency (CF) and the minimum threshold (MT). White stars represent minimum and maximum frequency measured 10 dB above MT. **d** Dot raster display and post-stimulus time histogram (red curve) of a response of the neuron shown in **b** to the CF at 10 dB above MT. **e** MT plotted as a function of CF. Marginal histogram above the scatterplot for CF was calculated with 5 kHz bin widths. Histogram of MT left to the scatterplot was calculated with 5 dB SPL bin widths. **f** Bandwidth (BW) measured 10 dB above MT plotted as a function of CF. Histogram of BW was calculated with 5 kHz bin width. **g** Response duration measured in each unit at 10 dB above MT at CF plotted as a function of CF. Histogram of duration was calculated with 10 ms bins. **h** Response latency plotted as a function of CF. Histogram of latency was calculated with 5 ms bin widths. Number of neurons = 716 units



Electrophysiological recordings

Experiments were performed in a custom-built sound-attenuating anechoic chamber. Anesthetized bats were placed in a body mold made of soft plastic foam and the head was tightly affixed to the stereotaxic apparatus by a rod attached to a metal holder. Neuronal recordings were performed using silicon probes from Cambridge Neurotech (16 contacts \times 2 shanks per probe with 250 μ m between

shanks and 50 μ m spacing between contact sites along each shank). Each shank had a thickness of 15 μ m. Using a micromanipulator system (MX7600R, Siskiyou Corp., OR, USA), probes were positioned perpendicular to the pial surface based upon landmarks and stereotaxic coordinates, and then inserted slowly into the brain through the intact dura mater to a depth of approximately 900 ± 50 μ m at the deepest contact point. Neuronal data were acquired with an OmniPlex D Neural Data Acquisition System recording

system (Plexon) at a sampling rate of 40 kHz (per channel) and 16-bit precision. Synchronization between the neural recordings and acoustic stimulus broadcasts was achieved with a TTL pulse output from the National Instrument card and recorded on one of the analog channels of the Plexon data acquisition system.

Analysis of neuronal recordings

Responses were analyzed offline using custom-made MATLAB scripts. The raw signal was digitally bandpass filtered offline (elliptic, second order) between 500 and 3000 Hz to obtain the spike activity. We used a threshold of 2.5 times the standard deviation of the baseline noise (30 repetitions of acoustic stimuli using a dead time of 100 ms) for spike detection. From the raster plots, representing the spike time versus the trial number, we measured the number of spikes in a window of 100 ms after the stimulus onset for each frequency-level combination. Frequency response areas (FRAs) were visualized as filled contour plots (contourc function, Matlab). From these, we calculated threshold curves as 25% of the maximum response. For each response, we calculated the minimum threshold (MT), characteristic frequency (CF) (i.e., the frequency and level at the lowest tip of the threshold curve), the minimum and maximum frequencies and the bandwidth of the tuning curve 10 dB above MT. We also measured the response duration in the post-stimulus time histogram of the response at CF at 10 dB above MT. Response duration was defined as the timespan between when the response first surpassed and then fell below 25% of the peak. The time at which the response reached 25% of the peak was considered the response latency.

A direction selectivity index (DSI) was calculated to quantify FM direction selectivity (O'Neill and Brimijoin 2002; Razak and Fuzessery 2006, 2008; Morrison et al. 2018). The formula used was:

$$DSI = (D - U) / (D + U),$$

where D and U are the maximum response magnitudes for downward and upward sweeps, respectively. The DSI was not necessarily calculated at the same sweep rate for the two directions because the maximum responses sometimes occurred at different durations for the two sweep directions. The DSI of each neuron was calculated using upward and downward sweeps of the same bandwidth. Values of DSI can range between -1 and $+1$, with more positive values indicating higher selectivity for the downward direction. DSI values > 0.6 show that the maximum response to the upward sweep was $\geq 75\%$ lower than the maximum response to the downward sweep.

Delay response areas (DRA) were visualized as filled contour plots using the `contourf` MATLAB function.

Threshold curves were calculated from DRAs as 50% of the maximum response. The characteristic delay (CD) was calculated as the delay at the lowest level sufficient for reaching 50% of the maximum spike count. The bandwidth of responses was calculated as the difference between maximum and minimum delay calculated in the threshold curve at 10 dB above the minimum level of the second FM eliciting a response.

For each bat, coordinates of the recording sites in relation to a branch of the median cerebral artery were measured using a calibrated micromanipulator (MX7600R, Siskiyou Corp.). All cortices were aligned together for the construction of composite maps using the branches and the median cerebral artery to determine the orientation of the ordinate axis of the bi-dimensional Cartesian space of analysis.

Results

Localization of the primary auditory cortex and basic response properties

Units responding to acoustic stimuli were found at parieto-temporal portions of the neocortex of *Tadarida brasiliensis*. The most consistent external features delineating the location of primary auditory cortex (AC) in bats are the middle cerebral artery and its dorsal branches (Dear et al. 1993a; Macías et al. 2009). The primary auditory cortical area as defined by neuronal responses to pure tones was found to cover a rostro-caudal distance of about 2500 μm and had a dorso-ventral extension of about 1600 μm in the lateral view (Fig. 1b).

Extracellular recordings in response to pure tones were derived from a total of 716 units from five bats. Because of technical reasons, we were only able to explore the left hemisphere. The number of units recorded per bat ranged from 59 to 258 per bat. Recording depths of units derived from orthogonal electrode penetrations were in the range of 250–1054 μm from the cortical surface. A typical frequency response area (FRA) with its corresponding frequency tuning curve, calculated as 25% of the maximum response, is represented in Fig. 1c. In this example, the white circle indicates the measured characteristic frequency (CF) and the minimum threshold (MT), while the white stars represent minimum and maximum frequency. Figure 1d shows the dot raster display (black dots) and the post-stimulus time histogram (PSTH, red line) for the response at the CF and 10 dB above the MT for the unit represented in Fig. 1c. We measured the response latency as the time the peristimulus time histogram (PSTH) reached 25% of its maximum. The difference between the response offset (time the PSTH falls down to 25% of its maximum) and latency rendered the response duration.

As shown in the vertical histogram in Fig. 1e, CFs of units ranged from 15 to 70 kHz ($n=716$ units, 25 kHz; interquartile range 15–35 kHz). Fifty percent of the units (363 of 716) had CFs between 20 and 30 kHz, i.e., in the range of the dominant frequencies of the echolocation pulses of *T. brasiliensis*. MT in the AC ranged from 20 to 70 dB SPL. The distribution of MT at CF showed two peaks with a first maximum at 40 dB SPL and second at 60 dB SPL (horizontal histogram in Fig. 1e). The lowest MT of ~20 dB SPL were measured at 15–25 kHz. At CFs higher than 25 kHz, we observed an increase of the neuronal MT with CF. On the basis of all the thresholds data from the four bats, a neural audiogram was calculated (continuous red line in Fig. 1e). The frequency range of 15–70 kHz was subdivided into classes of 5 kHz. Within each frequency class, the five lowest MTs were averaged. Based on the resulting means, the frequency threshold curve was drawn. The audiogram has a marked minimum of sensitivity at 20 kHz.

Bandwidth values covered a range between 5 and 41 kHz ($n=716$, median = 15.6 kHz; interquartile range 5–25 kHz). The distribution showed a peak around 15 kHz (Fig. 1f). Narrower bandwidths are found in units with CFs at 15–20 kHz (Fig. 1f) and increased as CF increased.

Units often exhibited onset responses to pure tones. The response duration to a 10 ms pure tone at 10 dB above MT at CF was determined in 697 units and ranged from 2 to 50 ms (Fig. 1g, median = 14 ms; interquartile range 5–30 ms). There was no clear relationships between CF and response duration. Response latency was measured in 697 cortical units and ranged between 10 and 44 ms (Fig. 1h, median = 17 ms; interquartile range 15–25 ms). There was a weak correlation (Pearson correlation, $R = -0.16$, $p < 0.05$) between latency and CF, where longer latencies were found in units with lower CF.

Figure 2a shows a composite map with data from the five bats depicting the organization of CFs within layer IV (450–600 μm from the cortical surface) of the AC of *T. brasiliensis* (Macias et al. 2019). In the frequency representation maps, a general tonotopy was found with low frequencies represented caudally and high frequencies represented more rostrally in all five sampled individuals (Fig. 2a). There is a frequency gradient of caudally located low CF (blue colors) to rostrally higher CF (brown colors). To quantify the tonotopy, we plotted the CF versus the rostro-caudal distance of the AC (Fig. 2b) and calculated the correspondent correlation coefficient (R , Pearson correlation). The correlation coefficient was significantly negative between CF and the rostro-caudal axis with a value of -0.6 ($p < 0.05$). There was not a clear topographical organization for MT as that shown for CF. However, lower MTs were found in the cortical areas tuned to CF between 20 and 25 kHz and higher MTs for areas tuned to higher CFs (Fig. 2c). Furthermore, there was a weak correlation between rostro-caudal distance and MT

(Fig. 2d, $R = -0.33$; $p < 0.05$). We did not observe any clear topography distribution for bandwidth, latency and response duration was not evident (Fig. 2e, g, i). There was no significant correlation between these basic response properties and the rostro-caudal axis (Fig. 2 f, h, j).

Selectivity to direction of frequency-modulated sweeps

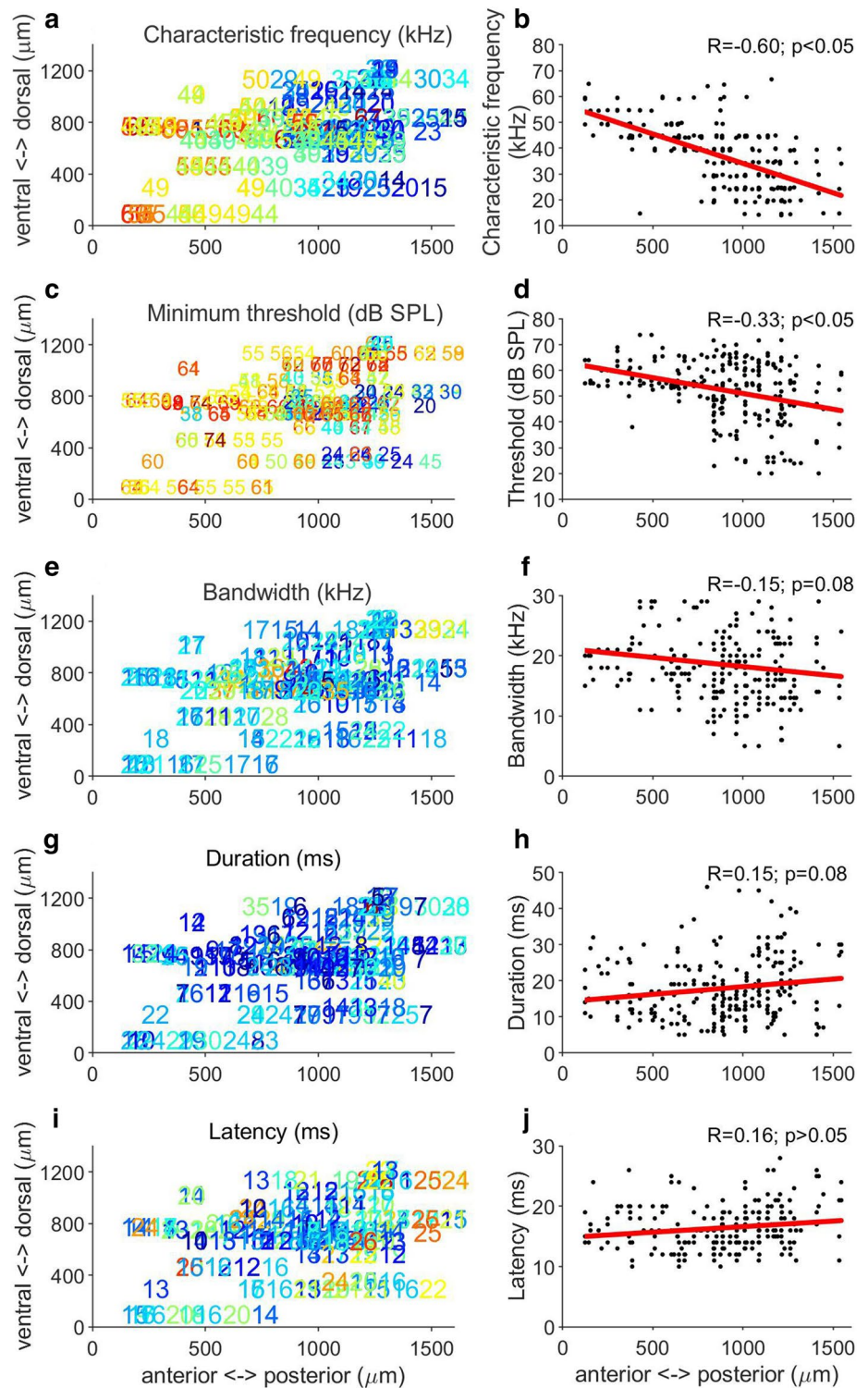
We determined FM direction selectivity by recording the responses to FM sweeps of various durations (1–50 ms) and a constant bandwidth of 50 kHz. We plotted the selectivity of a neuron as a function of FM rate (kHz/ms). FM direction selectivity was determined in 373 units of three bats. In these units, CFs ranged between 20 and 50 kHz. From these, 56% (208/373) of the units were selective for the downward direction of the FM sweep. Direction-selective neurons were defined as those in which upward sweeps elicited a response that was $< 25\%$ of the response to a downward sweep with the same bandwidth. The response of one example neuron in shown in Fig. 3a–d. This cortical neuron exhibited a direction selectivity index (DSI) value between 0.7, demonstrating strong selectivity for the downward FM sweep direction. In 164 units (43%), upward sweeps elicited a response that was $> 25\%$ of response to the downward sweep (Fig. 3e–h). No significant differences in DSI were found across different CF ranges (t test, $P > 0.05$ for all pairs), suggesting that most neurons prefer the downward sweep direction, regardless of frequency tuning characteristics. The distribution of DSI in the cortical units is shown in Fig. 4a. There was no clear relation between CF and DSI (Fig. 4b).

The composite map constructed out of the 247 neurons, recorded at cortical depths between 450–600 μm , from the AC of three bats is represented in Fig. 4c. There was no clear topographical distribution of DSI in the primary auditory cortex. There was no correlation between DSI and the anterior–posterior cortical axis, although lower DSI, indicating neurons selective to upward FM sweeps, are found in more posterior locations (Fig. 4d).

Echo-delay tuning

Delay selectivity was studied in 372 neurons in the auditory cortex of three bats, using pairs of artificial FM stimuli. Delay selectivity was found in 150 (40%). Figure 5 shows the response of two example neurons to FM–FM pairs, with CDs of 4 ms (Fig. 5a, b) and 8 ms (Fig. 5c, d). All delay-tuned neurons started to fire only after the presentation of the echo and the latency unequivocally increased with the echo delay. An example response is shown in Fig. 6a. We measured the slope of the relationship between the response latency and echo-delay at an echo amplitude 10 dB above the echo

Fig. 2 Topographic representation of response properties and their distribution along the rostro-caudal axis. **a, b** Characteristic frequency (CF). **c, d** Minimum threshold (MT). **e, f** Bandwidth, measured 10 above MT (BW). **g, h** Response latency. **i, j** Response duration



amplitude threshold. In all 150 neurons, this slope was higher than 1 (Fig. 6b, mean = 1.45 ± 0.23 ms/ms_{delay}). This indicates that in all 150 neurons, the response latency increases with echo delay and that the response is locked to the echo. CDs ranged from 4 to 16 ms, with the highest percentage of neurons (60/150, 40%) having

CDs of 4 ms (Fig. 6c). Response bandwidth was linearly correlated with the CD ($R = 0.62$, Fig. 6d). The echo-delay receptive field of the neurons, in contrast with that reported in the AC of other bat species (Hagemann et al. 2009, 2011; Hechavarría et al. 2013a, b), was not tilted. This CD remained constant with changing echo level.

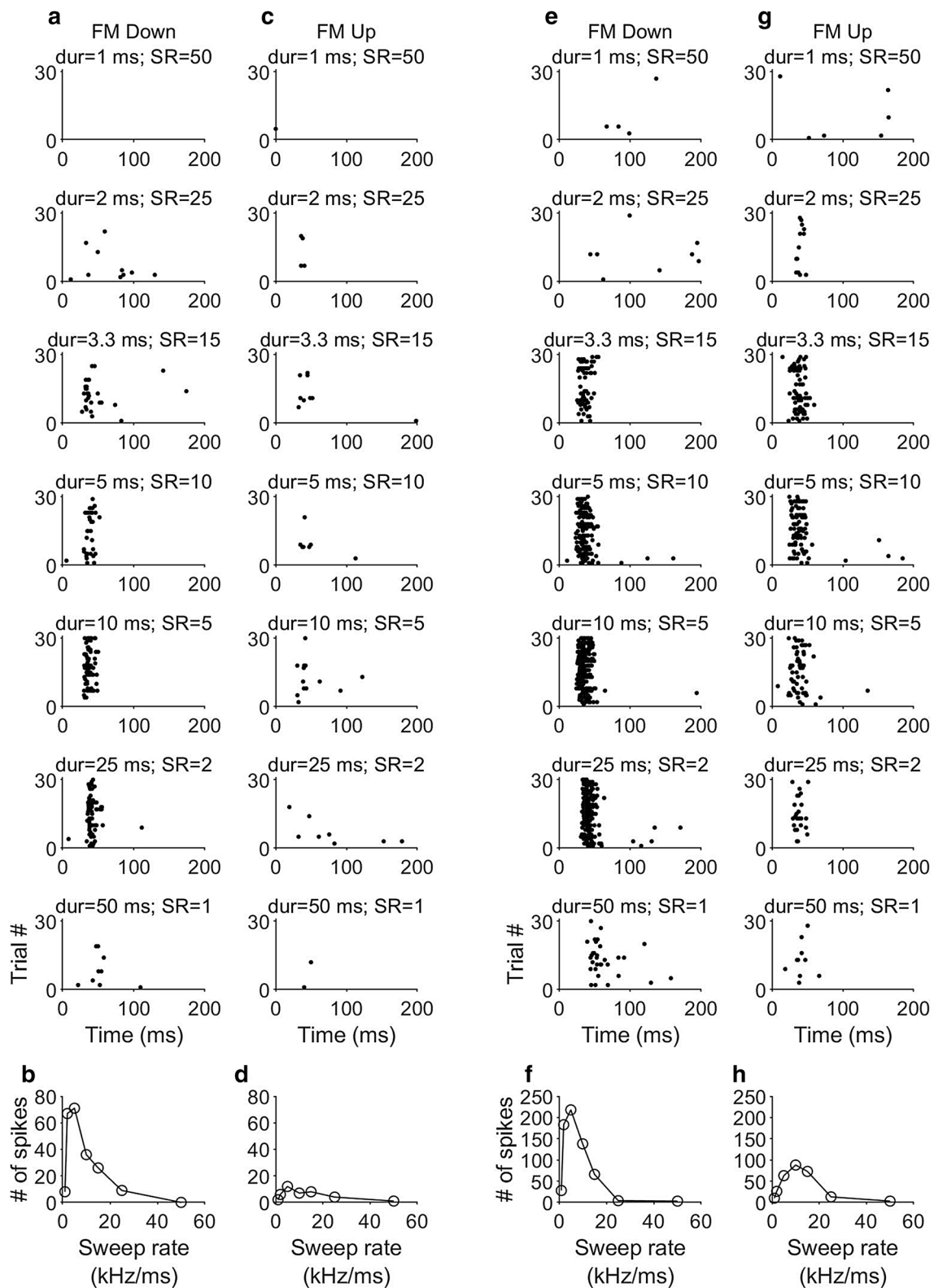


Fig. 3 Selectivity to FM sweep direction. **a–d** Example of a neuron sensitive to downward FM sweeps. **a** Dot raster plot of the response of a cortical neuron to downward FM sweeps of different sweep rates. **b** Number of spikes as a function of the sweep rate in the response shown in **a**. **c** Dot raster display of the same neuron in response to

upward FM sweeps with different sweep rates. **d** Number of spikes as a function of the sweep rate in the response shown in **c**. **e–h** Example neuron responding to both downward FM sweeps (**e–f**) and upward FM sweeps (**g–h**)

Fig. 4 Direction selectivity index. **a** Distribution of direction selectivity index (DSI) in 373 cortical neurons. **b** DSI as a function of the characteristic frequency. **c** Topographic representation of the DSI. **d** DSI as a function of the anterior–posterior axis

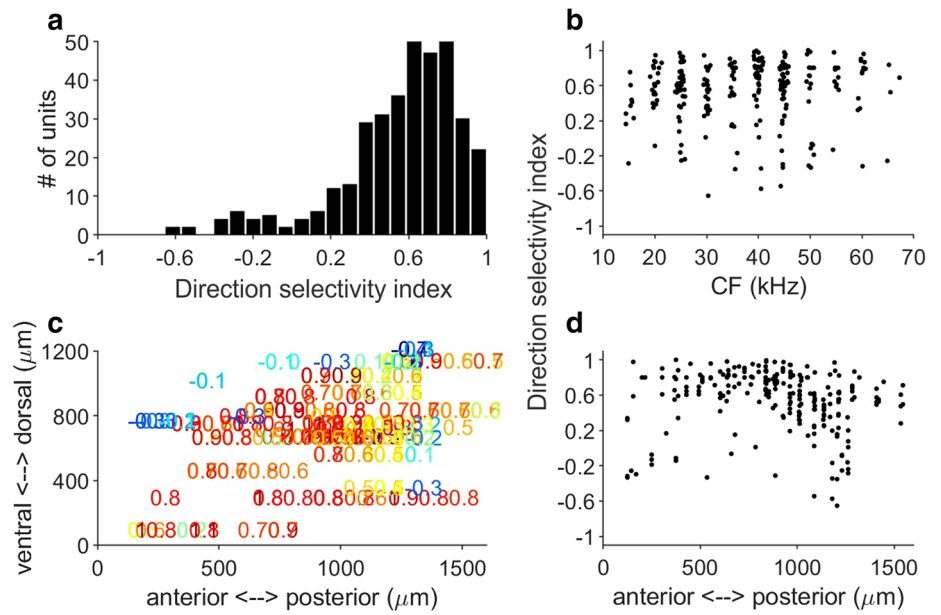
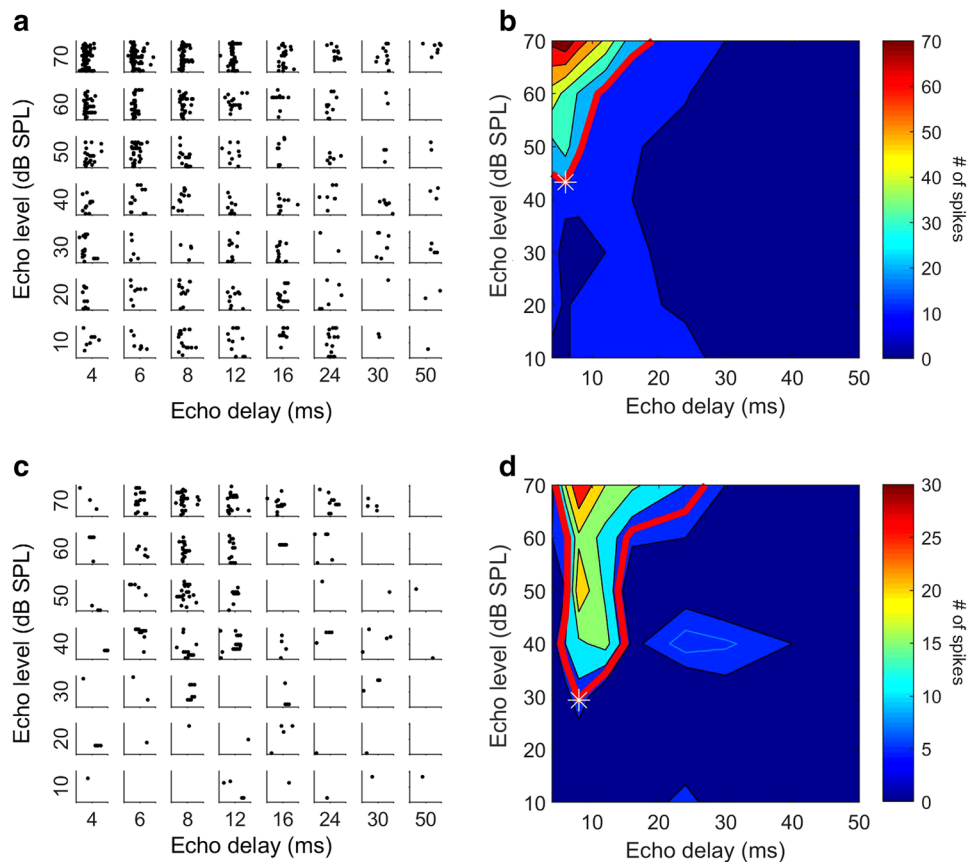


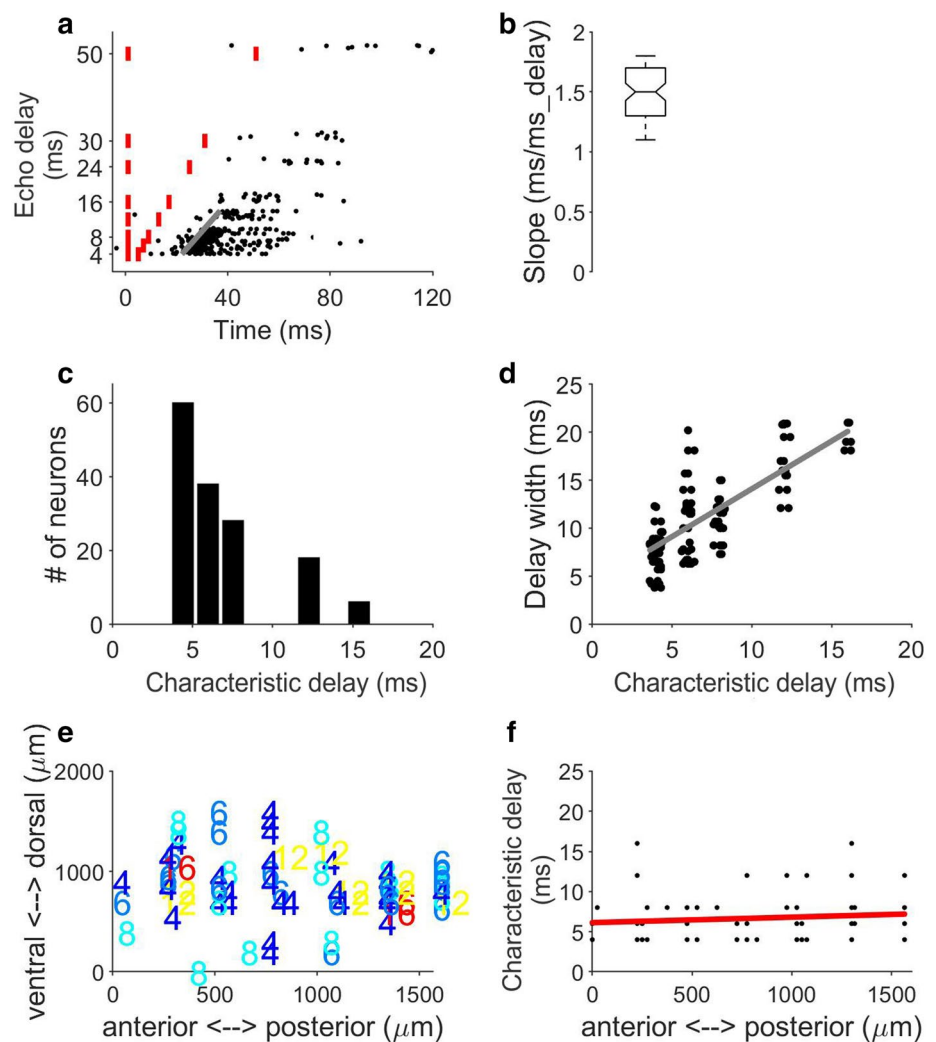
Fig. 5 Examples of two echo-delay-tuned neurons. **a, c** Dot raster display of the response to each combination of echo level and echo delay. **b, d** Delay response area and delay-tuning curve (red line) calculated as 25% of the maximum activity



A topographical organization of neurons according to the CD was not evident in the AC of the free-tailed bat. Delay-sensitive neurons were intermingled throughout the tonotopically organized area (Fig. 6e). There was

no evidence of any biases in distribution or correlation between CD and position along the anterior–posterior axis of the AC (Fig. 6f).

Fig. 6 Properties of echo-delay-tuned neurons. **a** Dot raster display of the response pattern of one neuron at an echo level 10 dB above the minimum echo amplitude. Red vertical lines indicate the temporal position of the FM pulses. Dots represent the spike times relative to the onset of the pulse. The regression line calculated with the response latencies at different echo delays is shown in gray. **b** Latency slope measured in the responses at different echo delays for 150 echo-delay neurons. A box and whisker plot shows the median (50th percentile) as a solid red line inside the box delimited by the 25th and 75th percentiles with whiskers extending to the 10th and 90th percentile. **c** Distribution of characteristic delays (binwidth = 4 ms). **d** Delay width as a function of CD ($n = 150$ neurons). **e** Topographic representation of the CD. **f** CD as a function of the anterior–posterior axis



Discussion

Topography and audiogram of the auditory cortex

The AC in the Mexican free-tailed bat shows an orderly tonotopic gradient with low frequencies located caudally and high frequencies rostrally, as assessed with multiunit activity responses. This orientation of the tonotopic axis is in accordance with findings in the tree shrew (Oliver et al. 1976), the rat (Horikawa et al. 1988), the gerbil (Scheich et al. 1993; Thomas et al. 1993), the dog (Tunturri 1962), the cat (Reale and Imig 1980), the marsupial northern native cat (Aitkin et al. 1986a), the house mouse (Stiebler et al. 1997) and bats such as *Pteronotus parnellii* (Suga and Jen 1976), *Eptesicus fuscus* (Jen et al. 1989; Dear et al. 1993a), *Rhinolophus ferrumequinum* (Ostwald 1984), *Rhinolophus rouxi* (Radtkeschuller and Schuller 1995), *Carollia perspicillata* (Esser and Eiermann 1999), *Molossus molossus* (Macías et al. 2009) and *Macrotus waterhousei* (Macías et al. 2014). However, it is different from the more ventral-to-dorsal ascending

tonotopic order of the AI in the cortex of the rabbit (McMullen and Glaser 1982), the ferret (Kelly et al. 1986; Shamma et al. 1993), and the brush-tailed possum (Gates and Aitkin 1982), or the reversed frequency arrangement in the squirrel (Merzenich et al. 1976), the guinea pig (Redies et al. 1989), or in monkeys [marmoset: Aitkin et al. (1986b); owl monkey: Imig et al. (1977); macaque monkey: Morel et al. (1993); Merzenich and Brugge (1973)].

In the AC of bats emitting CF-FM calls like the mustached bat, *Pteronotus parnellii*, *Rhinolophus rouxi* and *R. ferrumequinum*, there is an overrepresentation of neurons with characteristic frequencies close to the dominant frequency of their echolocation calls (O'Neill 1995; Ostwald 1980, 1984; Radtke-Schuller and Schuller 1995). In contrast, in FM bats a fairly uniform representation of the entire pulse bandwidth was reported in AC. In *Eptesicus fuscus* (Dear et al. 1993a), the frequency band of search calls (a single harmonic FM sweep dropping from 35 to 20 kHz, compared to 100–20 kHz multi-harmonic spectrum for approach phase calls) occupied roughly 24%

of the cortical area, and in *M. lucifugus* no evidence of overrepresentation at any particular frequency was evident (Wong and Shannon 1988). In this study, we found that the search-phase call bandwidths (30–20 kHz) were highly overrepresented, accounting for 50% of all cortical neurons. Similar results were reported for the bat *M. molossus*, a member of the same family as *T. brasiliensis*, for which 49% of the neurons in the AC showed characteristic frequencies in the range of that species' search-phase echolocation calls (Macías et al. 2009). This pattern may be correlated with the fast flight speeds and high-altitude hunting styles of these bats, which rely on comparatively low frequency and long duration pulses for detecting prey from long distances. The neural audiogram from the AC of *Tadarida* (present study) can be described as U shaped with a marked minimum of sensitivity between 20 and 25 kHz, and the AC audiogram appears notably similar to neural audiogram derived from the inferior colliculus single units (Pollak et al. 1978) and from auditory brainstem responses (Smotherman and Bakshi 2019). In this study, we only used frequencies between 15 and 70 kHz. However, the neural audiogram showed many low threshold neurons at 15 kHz, suggesting that there is a low-frequency sensitivity. This finding also suggests that this species of bat may have substantial low-frequency hearing, implying that both echolocating and non-echolocating signals are represented in the primary AC. The Mexican free-tailed bat has a rich repertoire of communication calls (Schwartz et al. 2007; Bohn et al. 2008) and sensitivity to this vocalizations is worth to explore in future studies.

Parcellation of the auditory cortex in bats

A comparison of the AC in the free-tailed bat with other bat species is summarized in Fig. 7. There is a substantial amount of information about the extent and parcellation of the AC in bats. In bats like the mustached bat and the rufous horseshoe bat, both of which are highly specialized insectivorous CF–FM bats, multiple functionally defined fields are shown (Suga 1965; Suga and Jen 1976; Suga 1977; O'Neill 1995; Fitzpatrick et al. 1998a; Radtke-Schuller and Schuller 1995; Hagemann et al. 2009). In the FM bat *Carollia perspicillata*, there are six functional fields that follows the nomenclature used in mice (Esser and Eiermann 1999). Echo-delay-sensitive neurons can be located in dorsal areas of AC, like in *P. parnellii*, *P. quadridens*, *R. rouxi*, *C. perspicillata*, *P. discolor* (Suga and Jen 1976; O'Neill 1995; Fitzpatrick et al. 1998a, b; Radtke-Schuller and Schuller 1995; Hoffmann et al. 2008; Hechavarría et al. 2013a, b). In species with such dedicated delay-sensitive cortical fields, there is a gradient of increasing characteristic neuronal delay towards caudal parts of the AC. Thereby, a chronotopic representation of echo delay is created and hence target distance is established. If a bat approaches a target, and we assume a successive activation of neurons that have different characteristic delay or best delay due to the pulse–echo pairs of the final buzz, an activation wave may run from caudal to rostral in the chronotopic areas. On the other hand, echo-delay-tuned neurons can be found within the tonotopic framework of the primary AC where they are interspersed with neurons that are not delay-sensitive, like in the AC of *M. lucifugus*, *E. fuscus* (Wong and Shannon 1988; Dear et al. 1993a) and the free-tailed bat (this study). Cortical representation of target

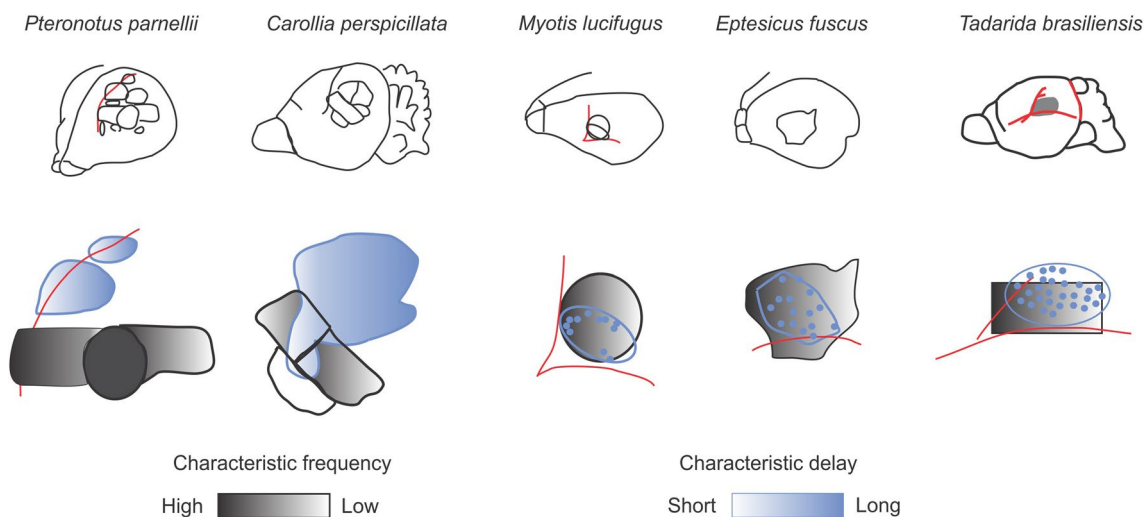


Fig. 7 Comparison of auditory cortex fields in bats. Tonotopy is indicated by grey shading. Echo-delay-sensitive areas are given in blue with chronotopic gradients in blue shading. *Pteronotus parnellii*

(Fitzpatrick et al. 1998a, b; Suga 2012); *Carollia perspicillata* (Hagemann et al. 2009; Esser and Eiermann 1999); *Myotis lucifugus* (Wong and Shannon 1988); *Eptesicus fuscus* (Dear et al. 1993a)

distance and acoustic scenes in these three latter bat species, which predominantly hunt in open uncluttered space, might be based on the ensemble coding of a large number of neurons (Dear et al. 1993b; Sanderson and Simmons 2002; Bates et al. 2011; Simmons 2012). The role of separate delay processing areas in the AC in the efficient extraction of spatial target distance information is still in debate.

The AC of the free-tailed bat contains a high percentage of neurons that respond preferentially to downward FM sweep. This bias to process downward FM sweeps seems to be a general feature of the AC of echolocating bats that rely on FM calls. In the AC of the pallid bat, most of the neurons are tuned either to the FM down of the frequency range of their echolocation calls or the FM down of the low-frequency noise used in the passive localization of the prey (Razak and Fuzessery 2002). This is different to that described in the mouse AC, where neurons with higher DSI, selective to FM down, are located in anterior cortical locations and there is a decrease of the DSI in the posterior direction (Zhang et al. 2003).

There are extensive physiological data available about the ascending auditory pathways of the free-tailed bat (Pollak et al. 2011). However, nothing is known about the functional organization of their auditory cortex. In this study, we offer a detailed description of the AC in terms of their neuronal response properties and topography, with particular emphasis on the FM direction selectivity and the echo-delay selectivity. Their biosonar behaviors and diverse repertoire of social calls makes this species a compelling model for the study of general properties of auditory processing for vocal communication and biosonar specializations.

Acknowledgements All experiments were carried out according to the National Institutes of Health guidelines and were approved by the TAMU Institutional Animal Care and Use Committee. This work was supported by the U.S. Office of Naval Research Grant No. ONRN00014-17-1-2736. KB received the support from the Texas A&M Institute for Neuroscience.

Compliance with ethical standards

Conflict of interest The authors declare that they have no conflict of interest.

References

- Aitkin LM, Irvine DRF, Nelson JE, Merzenich MM, Clarey JC (1986a) Frequency representation in the auditory midbrain and forebrain of a marsupial, the northern native cat (*Dasyurus hallucatus*). *Brain Behav Evol* 29(1–2):17–28. <https://doi.org/10.1159/000118669>
- Aitkin LM, Merzenich MM, Irvine DRF, Clarey JC, Nelson JE (1986b) Frequency representation in auditory cortex of the common marmoset (*Callithrix jacchus jacchus*). *J Comp Neurol* 252(2):175–185. <https://doi.org/10.1002/cne.902520204>
- Andoni S, Li N, Pollak GD (2007) Spectrotemporal receptive fields in the inferior colliculus revealing selectivity for spectral motion in conspecific vocalizations. *J Neurosci* 27(18):4882–4893
- Bates M, Simmons J, Zorikov T (2011) Bats exploit echo harmonic structure to distinguish targets from clutter and suppress interference. *Science* 333:627–630
- Bohn KM, Schmidt-French B, Ma ST, Pollak GD (2008) Syllable acoustics, temporal patterns, and call composition vary with behavioral context in Mexican free-tailed bats. *J Acoust Soc Am* 124(3):1838–1848
- Dear SP, Fritz J, Haresign T, Ferragamo M, Simmons JA (1993a) Tonotopic and functional organization in the auditory cortex of the big brown bat, *Eptesicus fuscus*. *J Neurophysiol* 70(5):1988–2009
- Dear SP, Simmons JA, Fritz J (1993b) A possible neuronal basis for representation of acoustic scenes in auditory cortex of the big brown bat. *Nature* 364(6438):620
- Esser KH, Eiermann A (1999) Tonotopic organization and parcellation of auditory cortex in the FM-bat *Carollia perspicillata*. *Eur J Neurosci* 11(10):3669–3682
- Fitzpatrick DC, Olsen J, Suga N (1998a) Connections among functional areas in the mustached bat auditory cortex. *J Comp Neurol* 391(3):366–396
- Fitzpatrick DC, Suga N, Olsen J (1998b) Distribution of response types across entire hemispheres of the mustached bat's auditory cortex. *J Comp Neurol* 391(1):353–365
- Gates GR, Aitkin LM (1982) Auditory cortex in the marsupial possum *Trichosurus vulpecula*. *Hear Res* 7(1):1–11. [https://doi.org/10.1016/0378-5955\(82\)90078-8](https://doi.org/10.1016/0378-5955(82)90078-8)
- Hagemann C, Esser K-H, Kössl M (2009) Chronotopically organized target-distance map in the auditory cortex of the short-tailed fruit bat. *J Neurophysiol* 103(1):322–333
- Hagemann C, Vater M, Kössl M (2011) Comparison of properties of cortical echo delay-tuning in the short-tailed fruit bat and the mustached bat. *J Comp Physiol A* 197(5):605–613
- Hechavarría JC, Macías S, Vater M, Mora EC, Kössl M (2013a) Evolution of neuronal mechanisms for echolocation: specializations for target-range computation in bats of the genus *Pteronotus*. *J Acoust Soc Am* 133(1):570–578
- Hechavarría JC, Macías S, Vater M, Voss C, Mora EC, Kössl M (2013b) Blurry topography for precise target-distance computations in the auditory cortex of echolocating bats. *Nat Commun* 4:2587
- Hoffmann S, Firzlaff U, Radtke-Schuller S, Schweltnus B, Schuller G (2008) The auditory cortex of the bat *Phyllostomus discolor*: localization and organization of basic response properties. *BMC Neurosci* 9(1):65
- Horikawa J, Ito S, Hosokawa Y, Homma T, Murata K (1988) Tonotopic representation in the rat auditory cortex. *Proc Jpn Acad B* 64(8):260–263. <https://doi.org/10.2183/pjab.64.260>
- Imig TJ, Ruggero MA, Kitzes LM, Javel E, Brugge JF (1977) Organization of auditory cortex in the owl monkey (*Aotus trivirgatus*). *J Comp Neurol* 171(1):111–128. <https://doi.org/10.1002/cne.901710108>
- Jen PH-S, Sun X, Lin PJ (1989) Frequency and space representation in the primary auditory cortex of the frequency modulating bat *Eptesicus fuscus*. *J Comp Physiol A* 165(1):1–14
- Kelly JB, Judge PW, Phillips DP (1986) Representation of the cochlea in primary auditory cortex of the ferret (*Mustela putorius*). *Hear Res* 24(2):111–115. [https://doi.org/10.1016/0378-5955\(86\)90054-7](https://doi.org/10.1016/0378-5955(86)90054-7)
- Kössl M, Hechavarría J, Voss C, Macías S, Mora E, Vater M (2014) Neural maps for target range in the auditory cortex of echolocating bats. *Curr Opin Neurobiol* 24:68–75
- Kössl M, Hechavarría J, Voss C, Schaefer M, Vater M (2015) Bat auditory cortex—model for general mammalian auditory computation or special design solution for active time perception? *Eur J Neurosci* 41(5):518–532

- Ma T, French B, Page R, Pollak G (2004) The social communication calls and songs of Mexican free-tailed bats. *Assoc Res Otolaryngol Abs* 1093
- Macías S, Bakshi K, Smotherman M (2019) Laminar organization of FM direction selectivity in the primary auditory cortex of the free-tailed bat. *Front Neural Circuits* 13:76. <https://doi.org/10.3389/fncir.2019.00076>
- Macías S, Mora EC, Kössl M, Abel C, Foeller E (2009) The auditory cortex of the bat *Molossus molossus*: disproportionate search call frequency representation. *Hear Res* 250(1–2):19–26
- Macías S, Hechavarría JC, Cobo A, Mora EC (2014) Narrow sound pressure level tuning in the auditory cortex of the bats *Molossus molossus* and *Macrotus waterhousii*. *Hear Res* 309:36–43
- McMullen NT, Glaser EM (1982) Tonotopic organization of rabbit auditory cortex. *Exp Neurol* 75(1):208–220. [https://doi.org/10.1016/0014-4886\(82\)90019-X](https://doi.org/10.1016/0014-4886(82)90019-X)
- Merzenich MM, Brugge JF (1973) Representation of the cochlear partition on the superior temporal plane of the macaque monkey. *Brain Res* 50(2):275–296. [https://doi.org/10.1016/0006-8993\(73\)90731-2](https://doi.org/10.1016/0006-8993(73)90731-2)
- Merzenich MM, Kaas JH, Roth GL (1976) Auditory cortex in the grey squirrel: tonotopic organization and architectonic fields. *J Comp Neurol* 166(4):387–401. <https://doi.org/10.1002/cne.901660402>
- Morel A, Garraghty PE, Kaas JH (1993) Tonotopic organization, architectonic fields, and connections of auditory cortex in macaque monkeys. *J Comp Neurol* 335(3):437–459. <https://doi.org/10.1002/cne.903350312>
- Morrison JA, Valdizón-Rodríguez R, Goldreich D, Faure PA (2018) Tuning for rate and duration of frequency-modulated sweeps in the mammalian inferior colliculus. *J Neurophysiol* 120(3):985–997. <https://doi.org/10.1152/jn.00065.2018>
- O'Neill WE (1995) The bat auditory cortex. In: Popper AN, Fay RR (eds) *Hearing by bats*. Springer, New York, pp 416–480. https://doi.org/10.1007/978-1-4612-2556-0_9
- Oliver D, Merzenich M, Roth G, Hall W, Kaas J (1976) Tonotopic organization and connections of primary auditory cortex in the tree shrew, *Tupaia glis*. *Anat Rec* 184:491
- O'Neill WE, Brimijoin WO (2002) Directional selectivity for FM sweeps in the suprageniculate nucleus of the mustached bat medial geniculate body. *J Neurophysiol* 88(1):172–187
- Ostwald J (1980) The functional organisation of the auditory cortex in the CF-FM bat *Rhinolophus ferrumequinum*. In: Busnel R-G, Fish JF (eds) *Animal sonar systems*. Springer US, Boston, pp 953–955. https://doi.org/10.1007/978-1-4684-7254-7_66
- Ostwald J (1984) Tonotopic organization and pure tone response characteristics of single units in the auditory cortex of the Greater Horseshoe Bat. *J Comp Physiol A* 155(6):821–834. <https://doi.org/10.1007/bf00611599>
- Pollak G, Marsh DS, Bodenhamer R, Souther A (1978) A single-unit analysis of inferior colliculus in unanesthetized bats: response patterns and spike-count functions generated by constant-frequency and frequency-modulated sounds. *J Neurophysiol* 41(3):677–691
- Pollak GD, Burger RM, Klug A (2003) Dissecting the circuitry of the auditory system. *Trends Neurosci* 26(1):33–39
- Pollak GD, Xie R, Gittelman JX, Andoni S, Li N (2011) The dominance of inhibition in the inferior colliculus. *Hear Res* 274(1–2):27–39
- Radtke-Schuller S, Schuller G (1995) Auditory cortex of the rufous horseshoe bat: 1. Physiological response properties to acoustic stimuli and vocalizations and the topographical distribution of neurons. *Eur J Neurosci* 7(4):570–591
- Razak KA, Fuzessery ZM (2002) Functional organization of the pallid bat auditory cortex: emphasis on binaural organization. *J Neurophysiol* 87(1):72–86
- Razak KA, Fuzessery ZM (2006) Neural mechanisms underlying selectivity for the rate and direction of frequency-modulated sweeps in the auditory cortex of the pallid bat. *J Neurophysiol* 96(3):1303–1319
- Razak KA, Fuzessery ZM (2008) Facilitatory mechanisms underlying selectivity for the direction and rate of frequency modulated sweeps in the auditory cortex. *J Neurosci* 28(39):9806–9816
- Reale RA, Imig TJ (1980) Tonotopic organization in auditory cortex of the cat. *J Comp Neurol* 192(2):265–291. <https://doi.org/10.1002/cne.901920207>
- Redies H, Sieben U, Creutzfeldt OD (1989) Functional subdivisions in the auditory cortex of the guinea pig. *J Comp Neurol* 282(4):473–488. <https://doi.org/10.1002/cne.902820402>
- Sanderson MI, Simmons JA (2002) Selectivity for echo spectral interference and delay in the auditory cortex of the big brown bat *Eptesicus fuscus*. *J Neurophysiol* 87(6):2823–2834
- Scheich H, Heil P, Langner G (1993) Functional organization of auditory cortex in the mongolian gerbil (*Meriones unguiculatus*) II. Tonotopic 2-deoxyglucose. *Eur J Neurosci* 5(7):898–914. <https://doi.org/10.1111/j.1460-9568.1993.tb00941.x>
- Schwartz C, Tressler J, Keller H, Vanzant M, Ezell S, Smotherman M (2007) The tiny difference between foraging and communication buzzes uttered by the Mexican free-tailed bat, *Tadarida brasiliensis*. *J Comp Physiol A* 193(8):853–863
- Shamma SA, Fleschman JW, Wiser PR, Versnel H (1993) Organization of response areas in ferret primary auditory cortex. *J Neurophysiol* 69(2):367–383. <https://doi.org/10.1152/jn.1993.69.2.367>
- Simmons JA (2012) Bats use a neuronally implemented computational acoustic model to form sonar images. *Curr Opin Neurobiol* 22(2):311–319
- Simmons JA, Lavender W, Lavender B, Childs J, Hulebak K, Rigden M, Sherman J, Woolman B, O'Farrell MJ (1978) Echolocation by free-tailed bats (*Tadarida*). *J Comp Physiol A* 125(4):291–299
- Smotherman M, Bakshi K (2019) Forward masking enhances the auditory brainstem response in the free-tailed bat, *Tadarida brasiliensis*, during a critical time window for sonar reception. *J Acoust Soc Am* 145(1):EL19–EL24. <https://doi.org/10.1121/1.5087278>
- Stiebler I, Neulist R, Fichtel I, Ehret G (1997) The auditory cortex of the house mouse: left-right differences, tonotopic organization and quantitative analysis of frequency representation. *J Comp Physiol A* 181(6):559–571. <https://doi.org/10.1007/s003590050140>
- Suga N (1965) Functional properties of auditory neurones in the cortex of echo-locating bats. *J Physiol* 181(4):671–700
- Suga N (1977) Amplitude spectrum representation in the Doppler-shifted-CF processing area of the auditory cortex of the mustache bat. *Science* 196(4285):64–67. <https://doi.org/10.1126/science.190681>
- Suga N (2012) Tuning shifts of the auditory system by corticocortical and corticofugal projections and conditioning. *Neurosci Biobehav Rev* 36(2):969–988
- Suga N, Jen P (1976) Disproportionate tonotopic representation for processing CF-FM sonar signals in the mustache bat auditory cortex. *Science* 194(4264):542–544
- Thomas H, Tillein J, Heil P, Scheich H (1993) Functional organization of auditory cortex in the mongolian gerbil (*Meriones unguiculatus*) I. Electrophysiological mapping of frequency representation and distinction of fields. *Eur J Neurosci* 5(7):882–897. <https://doi.org/10.1111/j.1460-9568.1993.tb00940.x>
- Tunturri A (1962) Frequency arrangement in the anterior ectosylvian auditory cortex of dog. *Am J Physiol* 203:185–193
- Wong D, Shannon SL (1988) Functional zones in the auditory cortex of the echolocating bat, *Myotis lucifugus*. *Brain Res* 453(1):349–352. [https://doi.org/10.1016/0006-8993\(88\)90176-X](https://doi.org/10.1016/0006-8993(88)90176-X)
- Zhang LI, Tan AY, Schreiner CE, Merzenich MM (2003) Topography and synaptic shaping of direction selectivity in primary auditory cortex. *Nature* 424(6945):201

Publisher's Note Springer Nature remains neutral with regard to jurisdictional claims in published maps and institutional affiliations.